In Vitro Sustained Release of LMWH from MgAl-layered Double Hydroxide Nanohybrids

Zi Gu,[†] Anita C. Thomas,[‡] Zhi Ping Xu,[†,*] Julie H. Campbell,[‡] and Gao Qing (Max) Lu[†,*]

ARC Centre of Excellence for Functional Nanomaterials and Centre for Research in Vascular Biology, Australian Institute of Bioengineering and Nanotechnology, The University of Queensland, Brisbane QLD 4072, Australia

Received December 17, 2007. Revised Manuscript Received March 6, 2008

Magnesium-aluminum-chloride-layered double hydroxides (MgAl-Cl-LDHs) intercalated with low molecular weight heparin (LMWH) were prepared for the first time by the coprecipitation method and then characterized by XRD, elemental analysis, FTIR, SEM, and TEM. MgAl-LDH was studied as the drug carrier for LMWH, a widely used anticoagulant, in order to overcome some of its pharmaceutical limitations, such as its short half-life. In vitro release tests of LMWH-LDH in pH 7.4 PBS at 37 °C show a biphasic and sustained profile of LMWH anion release with ~20% in the first 12 h and another ~20% in the following 108 h. After release, the residue was characterized and dissolution−diffusion kinetic models fitted. The mechanism of MgAl-LMWH-LDH release is probably due to surface diffusion and bulk diffusion via anionic exchange of LMWH anions on or in the LDH with anions in the PBS solution.

Introduction

Layered nanomaterials have attracted considerable attention as effective drug release systems for some time.[1,2] Of these materials, layered double hydroxides (LDHs) have as the advantages of ease of preparation, low cost, good biocompatibility, low cytotoxicity, and full protection for the loaded drugs.[3]

LDHs, also known as hydrotalcite-like materials or anionic clays, can be found naturally as minerals and can also be readily synthesized. They consist of brucite-like layers containing hydroxides of metal cations (M^{2+} and M^{3+}), and in the gallery space there are exchangeable anions (A^{n-}) and a variable amount of water molecules. The substitution of M^{2+} by M^{3+} in the layers results in the positive charge, which is neutralized by the interlayer anion (A^{n-}). The chemical composition of LDHs can be represented by the general formula $[M^{2+}_{1-x}M^{3+}_{x}(OH)_2]^{x+}(A^{n-})_{x/n}\cdot mH_2O$, where $x = 0.2-0.33$, which means the Mg/Al molar ratio is ca. 2.0−4.0, and $m = 1 - 3x/2$.[4,5] To incorporate as many anions as possible, the LDH with Mg/Al atomic ratio ~2 should be prepared, which has the highest layer positive charge density.

Because of LDHs' anionic exchange capacity, many pharmaceutically active compounds with negative charge at the physiological pH have been intercalated into the LDH interlayers, in order to prolong drug action. These include the anticancer drug MTX[6] and anti-inflammatory drugs fenbufen,[7] diclofenac,[8] ibuprofen[9] and camptothecin.[10] Additionally, Zhang and co-workers intercalated captopril, an angiotension-converting enzyme−inhibitor, into MgAl-LDH and studied the structure, thermal property, and in vitro release behavior of MgAl-captopril-LDH in pH 4.60 and 7.45 phosphate buffered saline (PBS) solutions.[11] Tronto et al. reported the intercalation of citrate anions into MgAl-LDHs and subsequent release.[12]

As cardiovascular disease has been the number one cause of death globally according to statistics reported by World Health Organization, we chose the anticoagulant low-molecular-weight heparin (LMWH), a highly sulfated glycosaminoglycan, to intercalate into MgAl-LDHs. LMWH (molecular weight ~4−6 kD), is frequently used as an anticoagulant,[13–15] but has some pharmaceutical limitations,

* To whom correspondence should be addressed. Tel: 61-7-33463809. Fax: 61-7-33463973. E-mail: gordonxu@uq.edu.au (Z.P.X.); maxlu@uq.edu.au (G.Q.L.).

[†] ARC Centre of Excellence for Functional Nanomaterials, The University of Queensland.

[‡] Centre for Research in Vascular Biology, The University of Queensland.

(1) Xu, Z. P.; Zeng, Q. H.; Lu, G. Q.; Yu, A. B. *Chem. Eng. Sci.* **2006**, *61*, 1027.
(2) Choy, J. H.; Kwak, S. Y.; Jeong, Y. J.; Park, J. S. *Angew. Chem., Int. Ed.* **2000**, *39*, 4042.
(3) Xu, Z. P.; Lu, G. Q. *Pure Appl. Chem.* **2006**, *78*, 1771.
(4) Okamoto, K.; Sasaki, T.; Fujita, T.; Iyi, N. *J. Mater. Chem.* **2006**, *16*, 1608.
(5) Braterman, P. S.; Xu, Z. P.; Yarberry, F. Layered Double Hydroxides (LDHs). In *Handbook of Layered Materials*; Auerbach, S. M., Carrado, K. A., Dutta, P. K., Eds; Marcel Dekker: New York, 2004; pp 373−474..
(6) Oh, J. M.; Park, M.; Kim, S. T.; Jung, J. Y.; Kang, Y. G.; Choy, J. H. *J. Phys. Chem. Solids* **2006**, *67*, 1024.
(7) Li, B. X.; He, J.; Evans, D. G.; Duan, X. *Appl. Clay Sci.* **2004**, *27*, 199.
(8) Ambrogi, V.; Fardella, G.; Grandolini, G.; Perioli, L.; Tiralti, M. C. *AAPS PharmSciTech* **2002**, *3*.
(9) Ambrogi, V.; Fardella, G.; Grandolini, G.; Perioli, L. *Int. J. Pharm.* **2001**, *220*, 23.
(10) Tyner, K. M.; Schiffman, S. R.; Giannelis, E. P. *J. Controlled Release* **2004**, *95*, 501.
(11) Zhang, H.; Zou, K.; Guo, S. H.; Duan, X. *J. Solid State Chem.* **2006**, *179*, 1792.
(12) Tronto, J.; dos Reis, M. J.; Silverio, F.; Balbo, V. R.; Marchetti, J. M.; Valim, J. B. *J. Phys. Chem. Solids* **2004**, *65*, 475.
(13) Hull, R. D.; Pineo, G. F.; Raskob, G. E. *Haemostasis* **1998**, *28*, 8.
(14) Liautard, C.; Nunes, A. M. C.; Vial, T.; Chatillon, F.; Guy, C.; Ollagnier, M.; Descotes, J. *Ann. Pharmacother.* **2002**, *36*, 1351.
(15) Schulman, S. *N. Engl. J. Med.* **2003**, *349*, 675.

10.1021/cm703602t CCC: $40.75
Published on Web 05/20/2008

such as a short half-life (2−4 h),[16] low efficiency of cellular delivery[17] and lack of oral absorption,[18] thus requiring generally twice daily injections.[16] In this study we used LDH as a carrier for LMWH to overcome these pharmaceutical limitations. The strongly negative charge of LMWH makes it easier for LMWH to exchange with A^{n-} and intercalate into the LDH interlayer, and thus the intercalated LMWH can be protected and its half-life in plasma extended. As a consequence of intercalation, the loaded LMWH can be released in a sustainable way. Second, LDH nanoparticles are found to be quickly taken up by various cell lines,[19,20] so the LDH nanocarrier could enhance LMWH cellular uptake. Moreover, conjugation of a specific antibody, such as fibrin,[21] gemtuzumab,[22] and certolizumab,[23] onto the LDH nanoparticle surface could facilitate the target cellular delivery with high efficiency. Finally, LDH probably facilitates oral administration of LMWH, because of electrostatic interactions between positively charged LMWH-LDH nanohybrid particles and negatively charged mucus.[24]

In this paper, we report the intercalation of LMWH into MgAl-LDH using the coprecipitation method. The in vitro release tests of LMWH-LDH nanohybrids show that LMWH anions were released ∼20% in the first 12 h and another ∼20% in the following 108 h and the LMWH release involves dissolution−diffusion processes.

Experimental Section

Synthesis of Cl-Containing $Mg_{2.4}Al$-LDH. The $Mg_{2.4}Al$-Cl-LDH, named as Cl-LDH or pristine Cl-LDH, was prepared using a coprecipitation method.[25] A solution (40 mL) containing 0.17 M NaOH (Labscan, 99.0%) was added to a solution (10 mL) containing 0.3 M $MgCl_2 \cdot 6H_2O$ (Fluka, 98.0%) and 0.1 M $AlCl_3.6H_2O$ (Fluka, 99.0%) with vigorous magnetic stirring at room temperature for 10 min in a sealed container. The resultant suspension was separated and washed twice by centrifugation using deionized water (dH_2O, 18.2 MΩ cm). The slurry was then manually dispersed in 40 mL of dH_2O and hydrothermally treated in a 45 mL autoclave at 100 °C for 16 h. The Cl-LDH particles were collected via high speed centrifugation and dried at 50 °C for 48 h for characterization.

Synthesis of LMWH-Containing $Mg_{2.4}Al$-LDH. The $Mg_{2.4}Al$-LMWH-LDH hybrids with the desired LMWH loading (LMWHn-LDH, n = 10, 20, 50, or 100, meaning that 10, 20, 50, or 100% of the Cl^- anions in the pristine Cl-LDH were replaced by LMWH anions) were prepared using a similar coprecipitation method. For example, to make LMWH10-LDH, a solution (40 mL) containing 0.17 M NaOH (Labscan, 99.0%) and heparin sodium salt ($[Na^+LMWH^-]$ = 2.5 mM, MW = 4−6 kD, Fluka) was preheated at 60 °C for 10 min under N_2 and then a solution (10 mL) containing 0.3 M $MgCl_2.6H_2O$ (Fluka, 98.0%) and 0.1 M $AlCl_3.6H_2O$ (Fluka, 99.0%) was added with vigorous magnetically stirring, and heated at 60 °C for 1 h under N_2 (for LMWH100-LDH, 80 °C for 3 h used to complete intercalation). Samples were then processed as outlined in Synthesis of Cl-containing $Mg_{2.4}Al$-LDH section, including separation, wash, and hydrothermal treatment.

DMB-LMWH Assay.[26] The amount of LMWH in solution was estimated using the dimethylmethylene blue (DMB) assay. DMB reagent consists of 16 mg of 1,9-dimethylmethylene blue (Aldrich) dissolved in 5 mL of ethanol (ACR, spectrophotometric grade), 2 mL of formic acid (Ajax Finechem, 99%), and 2 g of sodium formate (Aldrich), being made up to 1 L with dH_2O and protected from light. DMB reagent (1 mL) was mixed with 4 mL of LMWH sample and the absorbance read as the ratio of absorbance at 550 to 610 nm in a UV−vis absorption spectrophotometer JASCO V-550. The concentration of LMWH was determined using a standard curve of known concentrations of LMWH.

To determine the amount of LMWH loaded into the LDH, we placed 20 mg of the nanohybrid in a 50 mL of volumetric flask and added 0.8 mL HCl (1.000 M, Ajax Finechem) to dissolve the LDH. The flask was sealed and allowed to stand still overnight at 50 °C and then topped with pH 7.4 PBS. The LMWH concentration was then determined using the DMB assay.

In Vitro LMWH Release Test from LMWHn-LDHs. LMWH20-LDH (50 mg) was suspended in 150 mL pH 7.4 (the pH of blood) PBS solution in a sealed flask and incubated in a water bath at 37 °C with gentle shaking. A 3.0 mL aliquot of the medium solution was withdrawn at predetermined time points and replaced with 3.0 mL of fresh PBS. The aliquot was centrifuged three times to ensure removal of all the LMWH-LDH nanohybrid particles. After 5 days of release, the content of LMWH in triplicate aliquot samples was determined using the DMB assay. LMWH100-LDH was similarly tested. A physically mixed powder of heparin sodium salt and pristine Cl-LDH in the 1/8 weight ratio, similar to the chemical composition of LMWH20-LDH, was used as a control.

After release, the LMWHn-LDH residue solid was collected, and then dried at 50 °C for 48 h. This residue was named LMWHn-LDH-RP and characterized as described in the Characterizations section.

LMWH Release Kinetics. Four dissolution−diffusion kinetic models were used to fit the in vitro LMWHn-LDH release profiles.[27−31]

(1) The zero-order model describes the dissolution process and can be generally expressed as

$$M_t - M_0 = -k_0 t$$

(2) The first-order model expresses the release from systems where dissolution rate depends on the LMWH amount in the LDH hybrids and can be generally written as

(16) Kaul, S.; Shah, P. K. *J. Am. Coll. Cardiol.* **2000**, *35*, 1699.
(17) Brito, L.; Amiji, M. *Int. J. Nanomed.* **2007**, *2*, 143.
(18) Hoffart, V.; Ubrich, N.; Simonin, C.; Babak, V.; Vigneron, C.; Hoffman, M.; Lecompte, T.; Maincent, P. *Drug Dev. Ind. Pharm.* **2002**, *28*, 1091.
(19) Choy, J. H.; Kwak, S. Y.; Park, J. S.; Jeong, Y. J. *J. Mater. Chem.* **2001**, *11*, 1671.
(20) Tyner, K. M.; Roberson, M. S.; Berghorn, K. A.; Li, L.; Gilmour, R. F.; Batt, C. A.; Giannelis, E. P. *J. Controlled Release* **2004**, *100*, 399.
(21) Thomas, A. C.; Campbell, J. H. *J. Controlled Release* **2004**, *100*, 357.
(22) Kratz, F.; Abu Ajaj, K.; Warnecke, A. *Expert Opin. Invest. Drugs* **2007**, *16*, 1037.
(23) Dinesen, L.; Travis, S. *Int. J. Nanomed.* **2007**, *2*, 39.
(24) Hoffart, V.; Lamprecht, A.; Maincent, P.; Lecompte, T.; Vigneron, C.; Ubrich, N. *J. Controlled Release* **2006**, *113*, 38.
(25) Rives, V. *Layered Double Hydroxides: Present and Future*; Nova Science Publishers: New York, 2001.
(26) Chandrasekhar, S.; Esterman, M. A.; Hoffman, H. A. *Anal. Biochem.* **1987**, *161*, 103.
(27) Li, Z. H. *Langmuir* **1999**, *15*, 6438.
(28) Yang, J. H.; Han, Y. S.; Park, M.; Park, T.; Hwang, S. J.; Choy, J. H. *Chem. Mater.* **2007**, *19*, 2679.
(29) Demirbas, E.; Kobya, M.; Senturk, E.; Ozkan, T. *Water SA* **2004**, *30*, 533.
(30) Kodama, T.; Harada, Y.; Ueda, M.; Shimizu, K.; Shuto, K.; Komarneni, S. *Langmuir* **2001**, *17*, 4881.
(31) Sparks, D. L. *Kinetics of Soil Chemical Processes*; Harcourt Brace Jovanovich Publishers: San Diego, 1989.

$$\log(M_t/M_0) = -k_1 t$$

(3) The parabolic diffusion model elucidates the diffusion-controlled release of LMWH from LDH system and the equation is as follows

$$(1 - M_t/M_0)/t = k_d t^{-0.5} + a$$

(4) The modified Freundlich model explains experimental data on ion exchange and diffusion-controlled process with the following equation:

$$(M_0 - M_t)/M_0 = k_m t^b$$

In these equations, M_0 and M_t are the amount of LMWH in the LDH hybrids at release time 0 and t, respectively, k the corresponding release rate constant, and a and b constants whose chemical significance is not clearly resolved.[31]

Characterizations. Powder X-ray diffraction (XRD) patterns were recorded on a Rigaku Miniflex X-ray diffractometer using Co Kα source (λ = 0.178897 nm) at a scanning rate of 0.02°/s (2θ) from $2\theta = 2°$ to $2\theta = 80°$. Fourier transform infrared (FTIR) spectra were obtained on a Nicolet 6700 FTIR using the KBr pellet technique (sample/KBr = 1/100 weight ratio) in the range of 4000−400 cm^{-1}, by accumulating 32 scans at a resolution of 4 cm^{-1}. Elemental analysis was performed using ICP-OES technique on a Varian axial Vista CCD Simultaneousin with wavelength used for Mg, Al, S, and P at 383.829, 237.312, 181.972, and 185.878 nm, respectively. The morphology of the LDH particles was examined by scanning electron microscopy (SEM) and transmission electron microscopy (TEM) in a JEOL FESEM 6300 and a Tecnai 20 FEGTEM, respectively. TEM images of LDH samples that were dispersed in 75% ethanol solution via ultrasonication for 1 h were taken at 160 kV with magnifications of 100 000−700 000.

Results and Discussion

Crystal Structure and Chemical Composition of LDH Compounds. The powder XRD patterns of LMWHn-LDH samples are compared with the pristine Cl-LDH pattern in Figure 1a. The patterns of all the LDHs are typical of lamellar materials, characterized with basal reflections, associated harmonics at low 2θ angles and weaker nonbasal reflections at higher angles.[32] The pristine Cl-LDH is well-crystallized, as reflected by the sharp (003) and (006) basal reflections as well as two well-separated (110) and (113) peaks. The (003) spacing of Cl-LDH is 0.77 nm (Figure 1b), the same as reported in the literature.[33] As more LMWH being intercalated, i.e. from LMWH10-LDH to LMWH100-LDH, the above two (003) and (006) peaks become weaker and broader, as clearly shown by the increase in the full width at half-maximum (fwhm) of the (003) peak (Table 1). The weaker and broader peaks suggest the lower crystallinity and reduced particle size of Cl-LDH crystallites according to Scherrer's equation.[34] Simultaneously, a new set of basal reflections (marked with # in Figure 1a) can be observed starting from LMWH20-LDH, and LMWH100-LDH only shows such a unique set of reflections, and thus these

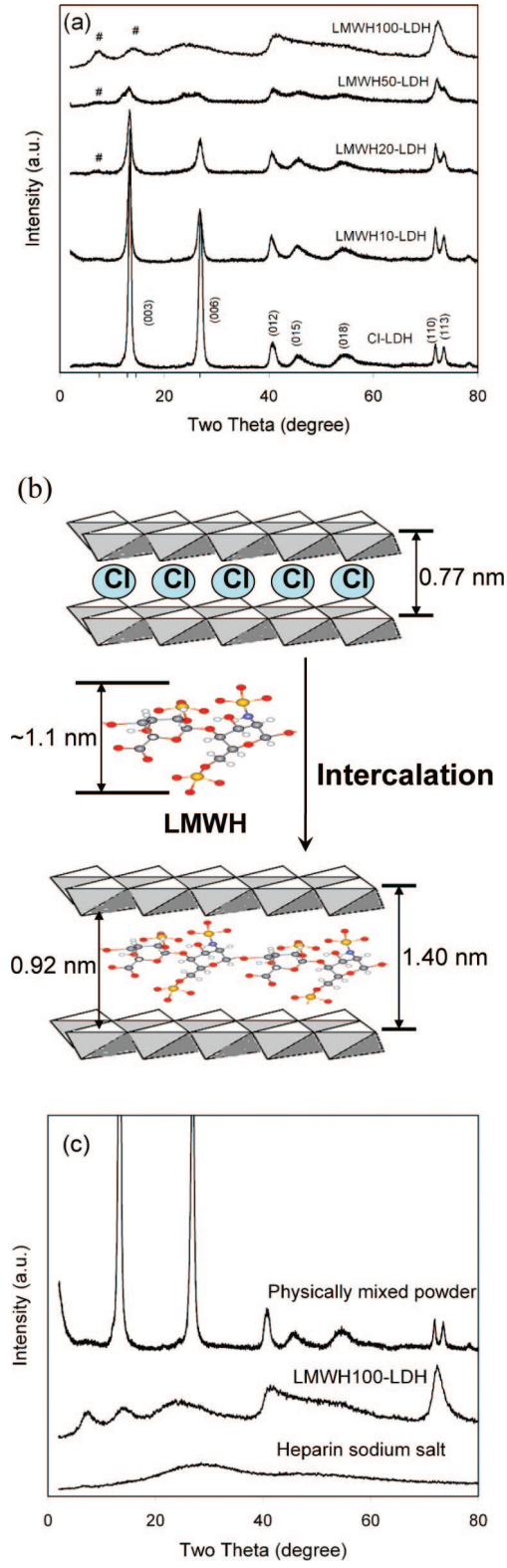

Figure 1. (a) Powder XRD patterns for pristine Cl-LDH and LMWHn-LDHs. # indicates the new set of basal diffractions attributed to the LMWH-intercalated LDH phase. (b) Schematic representation of LDH structure before and after LMWH intercalation. (c) Powder XRD patterns for physically mixed powder (heparin sodium salt/Cl-LDH = 1/8 weight ratio), heparin sodium salt alone, and LMWH100-LDH.

reflections could be attributed to LMWH-intercalated LDH phase, with the (003) spacing of 1.40 nm that is expanded by 0.63 nm compared with the pristine Cl-LDH (Figure 1b). Assuming a thickness of 0.48 nm for the brucite-like layer

(32) Wu, G. Q.; Wang, L. Y.; Evans, D. G.; Duan, X. *Eur. J. Inorg. Chem.* **2006**, *16*, 3185.
(33) Xu, Z. P.; Kurniawan, N. D.; Bartlett, P. F.; Lu, G. Q. *Chem.—Eur. J.* **2007**, *13*, 2824.
(34) West, A. R. *Solid State Chemistry and Its Applications*; John Wiley and Sons: New York, 1984.

Table 1. Full Width at Half-Maximum (fwhm) Values and Ratios of Key Elements of the LMWH-LDH Nanohybrid Particles (ICP Analysis)[a]

	fwhm	Mg (wt %)	Al (wt %)	S (wt %)	P (wt %)	Mg/Al	S/Al	P/Al
Cl-LDH	0.58	19.91	10.65	0.00	0.00	2.08	0.00	0.00
LMWH10-LDH	0.77	19.60	10.55	0.50	0.00	2.06	0.04	0.00
LMWH20-LDH	0.91	18.95	10.00	1.05	0.00	2.10	0.09	0.00
LMWH50-LDH	2.94	16.67	8.59	2.63	0.00	2.15	0.26	0.00
LMWH100-LDH		13.95	7.28	4.27	0.00	2.13	0.49	0.00
LMWH20-LDH-RP		16.50	9.50	0.55	4.40	1.93	0.05	0.40
LMWH100-LDH-RP		10.71	8.16	2.91	3.42	1.46	0.30	0.37

[a] Mg/Al, S/Al, and P/Al represent the molar ratio of Mg/Al, S/Al, and P/Al, respectively.

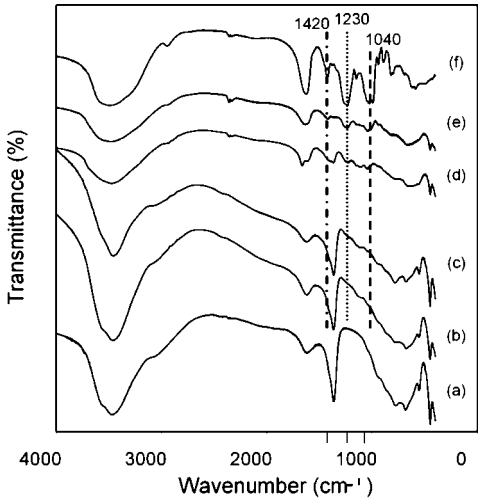

Figure 2. FTIR spectra for (a) Cl-LDH, (b) LMWH10-LDH, (c) LMWH20-LDH, (d) LMWH50-LDH, (e) LMWH100-LDH, (f) heparin sodium salt (MW = 4−6 kD).

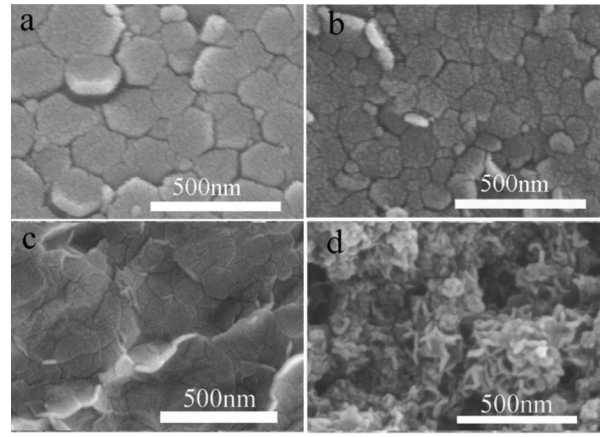

Figure 3. SEM images of (a) Cl-LDH, (b) LMWH20-LDH, (c) LMWH50-LDH, (d) LMWH100-LDH.

of LDH,[35] the gallery height in LMWH100-LDH is 0.92 nm, close to the thickness of the intercalated LMWH molecules (∼1.1 nm in a free state) when they adopt a helix oriented parallel to the basal plane of the LDH (Figure 1b). The reason for the small discrepancy between the experimental (0.92 nm) and estimated spacing (∼1.1 nm) is largely the spatial confinement caused by the strong electrostatic interactions between LMWH anions and LDH hydroxide layers. XRD patterns for heparin sodium salt and physically mixed powder show the diffraction peaks of the free LMWH anions/salt (Figure 1c). Heparin sodium salt alone and physically mixed powder exhibit no obvious diffraction peaks and a pattern similar to pristine Cl-LDH, respectively, whereas LMWH100-LDH diffracts differently, indicating that LMWH probably enters the LDH interlayer after the intercalation reaction, rather than simply binding to the LDH particle surface.

As listed in Table 1 (elemental analysis), the Mg/Al molar ratio in all LMWHn-LDH hybrids is in the range of 2.06−2.15, close to the nominal ratio 2.4. The ratio of S/Al atoms increases proportionally with the desired LMWH loading (10 to 100% range), indicating the presence of LMWH in and/or on the LDH particle.

The intercalation of LMWH anions into LDH interlayers is also suggested by the FTIR spectra for LMWHn-LDHs in comparison with pristine Cl-LDH or heparin sodium salt (Figure 2). The pristine Cl-LDH spectrum shows some peaks commonly appearing in MgAl-LDH spectra:[36,37] (1) the intense broadband around 3400−3500 cm^{-1} associated with stretching vibration of O−H in the brucite-like layer and water molecules; (2) the sharp band at 1363 cm^{-1} due to the contamination of CO_3^{2-} which is difficult to exclude from LDH synthesis; (3) the band at 554 cm^{-1} attributed to M−O and M−O−H stretching vibrations; and (4) the peak at 447 cm^{-1}, particularly characteristic of Mg_2Al-LDH materials.[33] These LDH feature peaks are also observed after incorporation of LMWH anions, but O−H bands become broader, CO_3^{2-} bands and M-O and M−O-H bands much weaker. In the spectra of all LMWHn-LDHs compared with that of heparin sodium salt, a few characteristic bands of LMWH are observed, attributed to the stretching vibration of C═O symmetric stretching (1420 cm^{-1}, C═O st_s), S═O antisymmetric (1230 cm^{-1}, S═O st_{as}), and symmetric stretching vibration (1040 cm^{-1}, S═O st_s).[37,38] Moreover, the $\Delta\nu(\nu_{as} - \nu_s = 190\ cm^{-1})$ value for LMWH100-LDH is close to that obtained from the spectrum of heparin sodium salt solution ($\Delta\nu = 210\ cm^{-1}$), which implies that LMWH interacts like a free-like anion with the LDH brucite-like layers, as does heparin sodium salt in solution.[39]

Morphology and Nanostructure. As can be seen in Figure 3, Cl-LDH and LMWHn-LDHs present compact and nonporous crystallites with a hexagonal plate-like shape when observed using SEM. With more LMWH being intercalated into the interlayer gallery, the particles become less regularly shaped. In particular, for LMWH50-LDH (Figure 3c), some well-formed hexagonally shaped larger particles are observed,

(35) Cavani, F.; Trifirò, F.; Vaccari, A. *Catal. Today* **2001**, *11*, 173.
(36) Xu, Z. P.; Saha, S. K.; Braterman, P. S.; D'Souza, N. *Polym. Degrad. Stab.* **2006**, *91*, 3237.
(37) Nakamoto, K. *Infrared and Raman Spectra of Inorganic and Coordination Compounds*; 5th ed.; John Wiley and Sons: New York, 1997.
(38) Yang, T.; Hussain, A.; Bai, S.; Khalil, I. A.; Harashima, H.; Ahsan, F. *J. Controlled Release* **2006**, *115*, 289.
(39) Gordijo, C. R.; Barbosa, C. A. S.; Ferreira, A.; Constantino, V. R. L.; Silva, D. D. *J. Pharm. Sci.* **2005**, *94*, 1135.

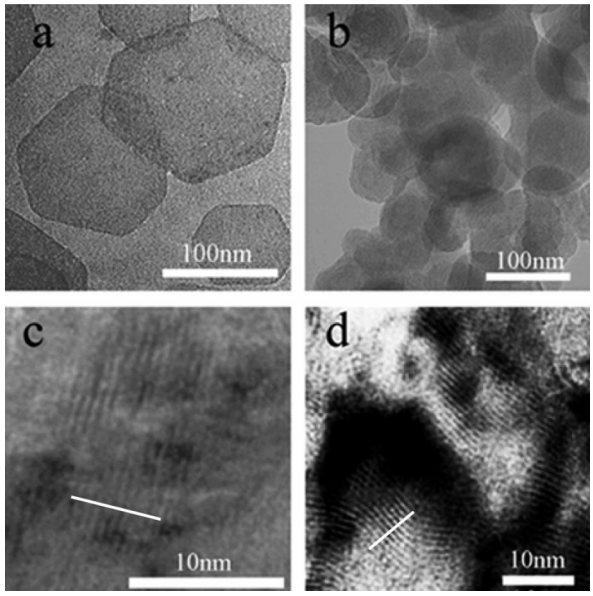

Figure 4. TEM images of (a, c) Cl-LDH, (b) LMWH100-LDH, (d) LMWH20-LDH. a and b (low-magnification images) show the lateral dimension of particles; c and d (high-magnification images) show the layered structure of particles, in which the white line indicates the 10 layer−interlayer units in 5 visual fields.

suggesting that the intercalation of LMWH anions influences the LDH crystallization behavior. The average lateral dimension of particles obviously decreases from ∼190 nm (Cl-LDH) to ∼90 nm (LMWH100-LDH) (images a and d in Figure 3). The particle size of LMWHn-LDH meets the requirement for administration by injection and makes LDH to be an effective LMWH carrier possible.

The morphology of individual nanohybrid particles is further examined using TEM (Figure 4). As a consequence of LMWH intercalation the LDH nanoparticle shape changes from regular hexagon to ellipse (images a and b in Figure 4). At higher magnification (images c and d in Figure 4), the layered structure of both Cl-LDH and LMWH20-LDH is clearly observed. The dark and bright stripes represent the mixed hydroxide layers and the interlayers with exchangeable organic ($LMWH^{n-}$) and inorganic (Cl^-, CO_3^{2-}) anions, respectively.[40,41] The average (003) spacing was calculated by measuring 10 repeated layer-interlayer units in 5 visual fields (images c and d in Figure 4). As shown in Figure 4c, the pristine Cl-LDH has an average (003) spacing of ∼0.65 nm, in line with the spacing determined using XRD (0.77 nm). The layered structure of LDH is still preserved after the incorporation of LMWH anions to form LMWH20-LDH (Figure 4d). The average (003) spacing of LMWH20-LDH is ∼1.00 nm, between 0.77 nm (Cl-LDH) and 1.40 nm (LMWH100-LDH) calculated from XRD data, and thus corresponding to partial intercalation. This is the direct evidence that shows the enlargement of interlayer distance is caused by the exchange of the larger LMWH anions with chloride ones.

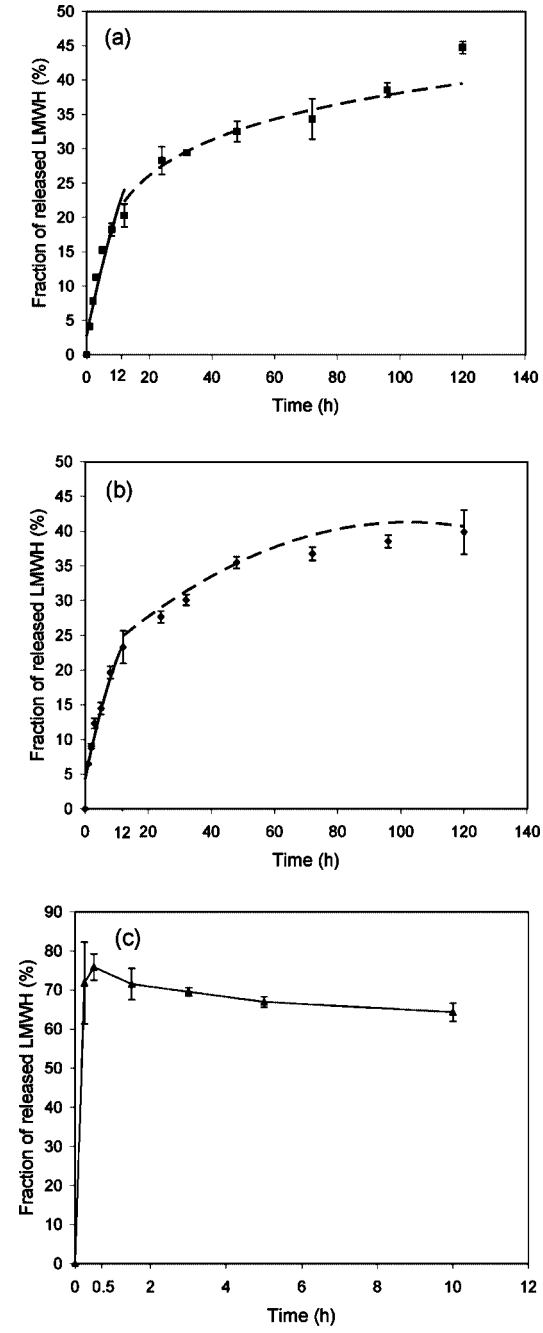

Figure 5. In vitro LMWH release curves from (a) LMWH20-LDH, (b) LMWH100-LDH, (c) physically mixed powder of heparin sodium salt and Cl-LDH (1/8 weight ratio). In a and b, the solid and dashed curves represent the modified Freundlich and parabolic diffusion model prediction, respectively.

In Vitro Drug Release of LMWHn-LDHs. The LMWH release profiles from LMWH20-LDH and LMWH100-LDH (i.e., the fraction of released LMWH vs the release time) are shown in Figure 5. LMWH20-LDH in pH 7.4 PBS has a gradual and biphasic release pattern (Figure 5a), with an early fast release of LMWH (20.3% of LMWH released after the first 12 h) followed by a relatively slower release (44.7% of LMWH released after 120 h). LMWH100-LDH shows a similar biphasic release pattern (Figure 5b), in which 23.3% of LMWH was released in the first 12 h and 39.9% in 120 h. Generally, LMWH release from LMWH-LDH nanohybrid particles takes a much longer time than the release of other small drugs from MgAl-LDH at pH 7−8 in the literature.

(40) Plank, J.; Dai, Z.; Andres, P. R. *Mater. Lett.* **2006**, *60*, 3614.
(41) Plank, J.; Keller, H.; Andres, P. R.; Dai, Z. M. *Inorg. Chim. Acta* **2006**, *359*, 4901.

Ambrogi and colleagues reported that 90% of diclofenac and 100% of ibuprofen were released after 9 h and 100 min, respectively,[8,9] while Li and colleagues established that 59% of fenbufen was released after 2 h.[7] Zhang et al. reported that 94.2% of captopril was released after 140 min.[11] The much more extended release period for LMWH to release from LDH nanohybrids is largely due to the strong electrostatic interactions between the positively charged LDH hydroxide layers and the negative charged LMWH anions in the LDH interlayer. Most drug molecules are singly or doubly charged anions, but LMWH is multianionic species, with ~20 OSO_3^- and ~10 COO^- in each molecule. Therefore this multianionic LMWH has much stronger electrostatic interactions with the positively charged LDH hydroxide layers, and can only be released when all the binding OSO_3^- and COO^- are replaced by phosphate/chloride anions. The biphasic and prolonged release profile resulting from a single dose of the nanohybrid could benefit therapeutic treatment, as the initial fast release quickly allows establishment of a therapeutic dose, and the subsequent sustained release allows maintenance of this dose over a long period of time.

In contrast with LMWHn-LDH, the physically mixed powder had a burst release of 75.9% within the first 30 min (as some LMWH molecules weakly electrostatic-interacted with the surface of the LDH particles), followed by a steady decline of LMWH in solution, with only 64.3% of LMWH in solution after 10 h (Figure 5c). The reintercalation of LMWH into LDH under 37 °C was confirmed by measuring the amount of LMWH remaining in the powder recovered after release. This release pattern deviates from the release of small drug molecules from LDH, where all of the drug molecules are released in a burst way, without obvious reintercalation.[9,12] The reintercalation of LMWH may also be attributed to its multianionic interaction with the hydroxide layers.

To understand the LMWHn-LDH release behavior, the resultant powder was recovered after the release test (120 h) and further characterized. XRD patterns for LMWHn-LDH-RP with reference to the original LMWHn-LDH are illustrated in Figure 6a. For LMWH20-LDH-RP, new peaks (marked as #) appear around $2\theta = 11.5$, 23.3, and 37.3°. The corresponding (003) spacing is calculated to be 0.89 nm, in agreement with 0.88 nm of phosphate-intercalated LDH reported previously.[42] These three peaks in LMWH100-LDH-RP are difficult to observe, probably due to their overlap with the basal diffraction peaks of LMWHn-LDH. The FTIR spectra of LMWHn-LDH-RP (Figure 6b) show bands characteristic of phosphate centered at 1100 cm^{-1}, assigned to δ(P-OH) and ν_3(P−O).[11,37,42,43] In the spectrum of LMWH100-LDH-RP, the intensity of S═O st_{as} band centered at 1230 cm^{-1} is reduced, indicating decrease in LMWH amount compared with the original LMWH100-LDH. From the ICP analysis for LMWHn-LDH-RP (Table 1), the amount of sulfur in LDH nanohybrids is reduced by 44.4% (LMWH20-LDH) and 38.8% (LMWH100-LDH) after release, in good agreement with the fraction of released LMWH (44.7% for LMWH20-LDH and 39.9% for LMWH100-LDH). A considerable amount of phosphate is detected after release (Table 1), suggesting the intercalation of phosphate anions in the LDH by replacing LMWH and chloride anions.[44] Moreover, the Mg/Al molar ratio drops from 2.1 to 1.93 (LMWH20-LDH release) and 1.46 (LMWH100-LDH release), due to Mg^{2+} leaking as well as dissolution of LDH hydroxide layers. Careful observation reveals that LMWH100-LDH dissolves more considerably than LMWH20-LDH, probably due to the poorer crystallization of LMWH100-LDH. The analysis of the collected LDH residues illustrates that the release of LMWH from LDH hybrids is mainly via exchange with phosphate anions as well as simultaneous dissolution of the LDH layers/edges.

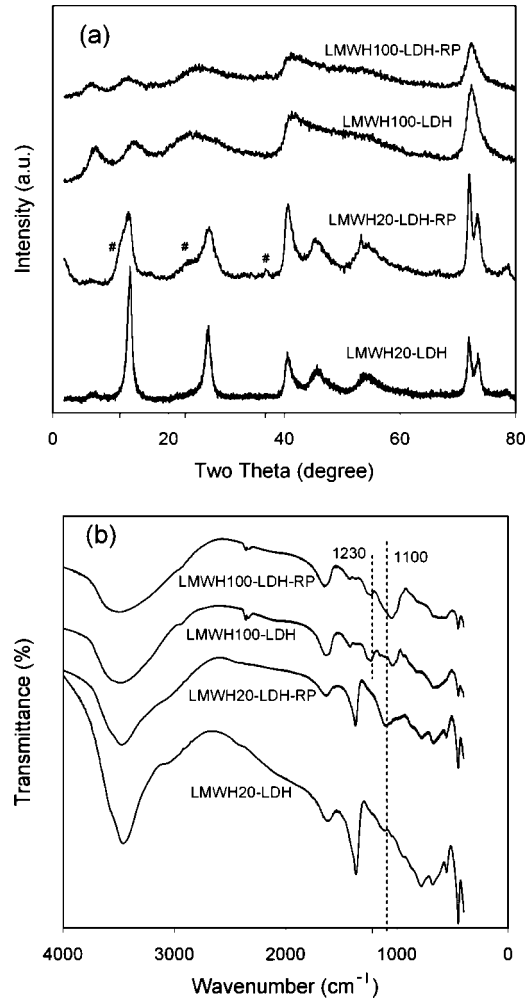

Figure 6. (a) XRD and (b) FTIR profiles for LMWH20-LDH-RP and LMWH100-LDH-RP with reference to LMWH20-LDH and LMWH100-LDH. # indicates the new set of basal diffractions attributed to the phosphate-intercalated LDH phase.

Release Models. To gain more insights into the mechanism of release, we applied four types of dissolution-diffusion kinetic models (zero-order, first-order, parabolic diffusion, and modified Freundlich model; Figure 7), and calculated the corresponding linear correlation coefficients (R^2) (Table

(42) Costantino, U.; Casciola, M.; Massinelli, L.; Nocchetti, M.; Vivani, R. *Solid State Ionics* **1997**, *97*, 203.
(43) Badreddine, M.; Khaldi, M.; Legrouri, A.; Barroug, A.; Chaouch, M.; De Roy, A.; Besse, J. P. *Mater. Chem. Phys.* **1998**, *52*, 235.
(44) Komarneni, S.; Newalkar, B. L.; Li, D.; Gheyi, T.; Lopano, C. L.; Heaney, P. J.; Post, J. E. *J. Porous Mater.* **2003**, *10*, 243.

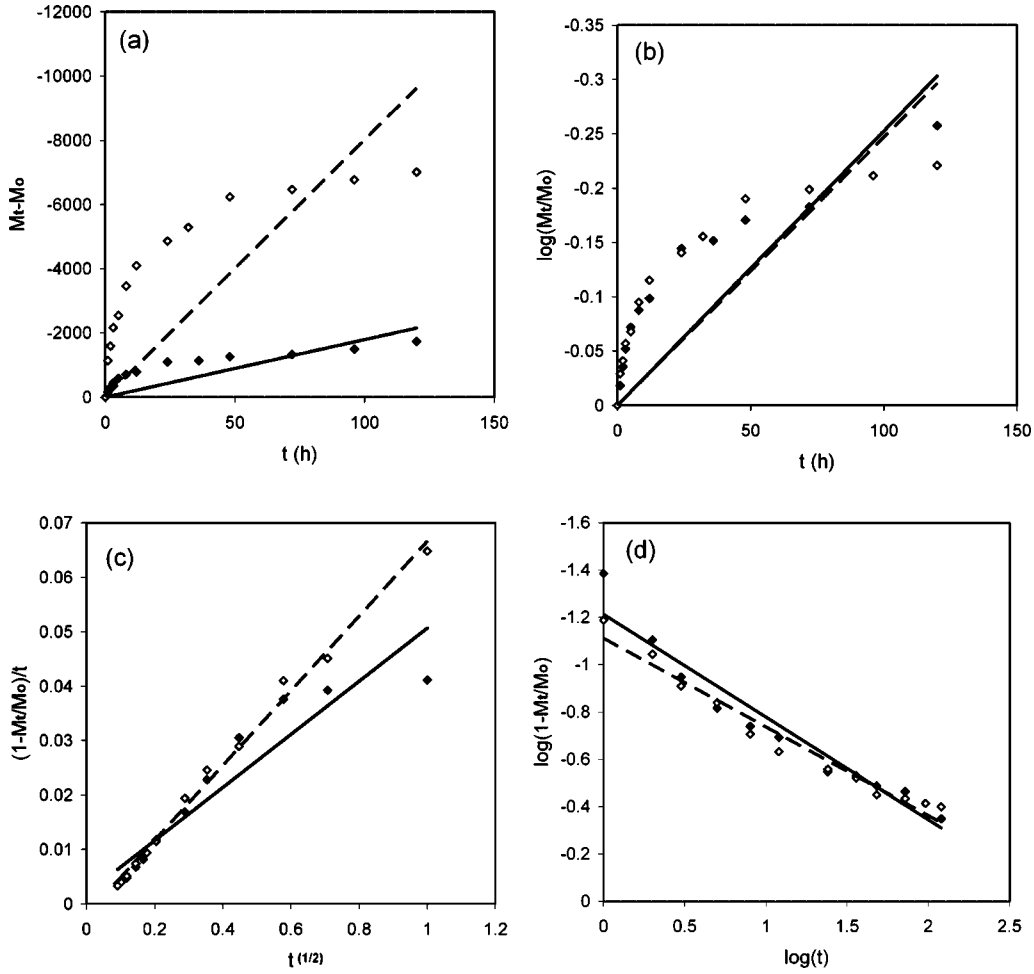

Figure 7. Plots of dissolution−diffusion kinetic models of (a) zero-order model, (b) first-order model, (c) parabolic diffusion model, (d) modified Freundlich model for the release of LMWH from LMWH20-LDH (filled diamonds) and LMWH100-LDH (open diamonds). The linear modeling is shown as the solid curve (for LMWH20-LDH) and the dashed curve (for LMWH100-LDH).

Table 2. Linear Correlation Coefficients (R^2) of the Dissolution−Diffusion Kinetic Models Applied to LMWH Release from LMWH20-LDH and LMWH100-LDH

	LMWH20-LDH			LMWH100-LDH		
kinetic models	I[a]	II[b]	W[c]	I[a]	II[b]	W[c]
zero-order model	0.7288		0.3684	0.7467		0.1045
first-order model	0.7748		0.5750	0.8095		0.3336
parabolic diffusion model	0.7805	0.9933	0.8957	0.9919	0.9949	0.9932
modified Freundlich model	0.9521	0.9599	0.9393	0.9932	0.9714	0.9632

[a] For release in 0−12 h. [b] For release in 12−120 h. [c] For the whole release process (0−120 h).

2). In general the zero- and first-order models are not suitable to explain the whole release of LMWH20-LDH or LMWH100-LDH, which is reflected by modeling data points that do not form a straight line (panels a and b in Figure 7) and small linear correlation coefficients ($R^2 = 0.10-0.58$) (column W of Table 2). The other two models fit the release data much better (panels c and d in Figure 7), with linear correlation coefficients of $R^2 = 0.90-0.94$ for release from LMWH20-LDH and 0.96−0.99 for release from LMWH100-LDH (Table 2).

A detailed examination of the data point distribution in Figure 7 suggests that the whole release process consists of two linear stages. In order to better simulate the LMWH release model, we applied the kinetic models as two separate stages, with stage I in 0−12 h and stage II in 12−120 h. Stages I and II for LMWH release from LMWH20-LDH and LMWH100-LDH are best fitted with the modified Freundlich and parabolic diffusion models, respectively, with a linear correlation coefficient of $R^2 = 0.95-0.99$. The kinetic model predicted profiles are shown in Figure 5. The modified Freundlich model describes heterogeneous diffusion from the flat surfaces via ion exchange, while the parabolic diffusion model describes intraparticle diffusion or surface diffusion.[28] These simulation results suggest that (i) the release at both stages is diffusion-controlled; (ii) within first 12 h (stage I), most LMWH anions on the surface of LDH particles diffuse into the medium solution via anion exchange; and (iii) at stage II, surface diffusion, but not the controlling step, is continuing; the controlling step is the LMWH anions diffusion from the inside to the surface of LDH particles, which takes a longer time than at stage I. This biphasic model prediction is consistent with the release process of LMWH from LDH nanohybrids. LMWH20-LDH and LMWH100-LDH nanocrystallites are mostly 5−10 layers (5−15 nm thick and 50−150 nm wide; observed and calculated from SEM, TEM, and XRD results). There is ∼10−20% of LMWH on the surface or edge of the nanoparticle, which diffuses into solution via exchange with phosphate/chloride (stage I). Simultaneously, the bulk LMWH diffuses toward the edge/surface (intraparticle diffusion), together with the

leaking of Mg^{2+} and the dissolution of LDH hydroxide sheets, resulting in continuous release of LMWH from the nanohybrids (stage II).

Additionally, the kinetic model predictions suggest differences in the release of LMWH20-LDH and LMWH100-LDH. Both the parabolic diffusion and modified Freundlich models seem to well fit the whole release data for LMWH100-LDH ($R^2 = 0.96-0.99$). This may be related to the much smaller size of the LMWH100-LDH nanohybrid particles (i.e., smaller lateral dimension). As smaller LDH particles provide more side edges/surfaces and shorter diffusion path, the bulk LMWH can more readily diffuse toward the edge/surface in a relatively continuous way even at the beginning of release.

Conclusions

MgAl-LDH nanohybrids intercalated with LMWH (MW = 4−6 kD) were for the first time synthesized using the coprecipitation method, and confirmed by XRD, elemental analysis, FTIR, SEM, and TEM. XRD patterns demonstrate smaller crystals and expanded (003) spacing (from 0.77 nm for Cl-LDH to 1.40 nm for LMWH100-LDH) due to LMWH intercalation, which is consistent with SEM and TEM observations. The elemental analysis from ICP indicates that the sulfur content increases as the LMWH nominal loading increases. FTIR spectra show the characteristic bands of LMWH (C═O st_s, S═O st_{as}, and st_s) in LMWHn-LDHs. LMWH anions were released from the LDH nanohybrid particles in a two-phased, prolonged and sustained way. The kinetic modeling by using four dissolution-diffusion kinetic models indicates that the LDH nanohybrids with low loading and high loading of LMWH (i.e., LMWH20-LDH and LMWH100-LDH) exhibit similar release behavior, mainly involving the surface diffusion and bulk diffusion of loaded LMWH. Overall, we have shown that LMWH can be stored in MgAl-LDH interlayers and sustainably released under simulated blood conditions, indicating that MgAl-LDH is a promising nanocarrier for LMWH.

Acknowledgment. This project was supported by ARC Centre of Excellence for Functional Nanomaterials (ARCCFN). The authors thank Mr. Yanan Guo and other members in the Centre for Microscopy and Microanalysis for their help in the microscopy study. The authors also extend thanks to Dr. Chenghua Sun for his contribution in LMWH molecular size estimation and Queensland Health Pathology and Scientific Services (QHPSS) for ICP analysis.

CM703602T